Chapter 1

Introduction

We come across the phenomenon of turbulence in our everyday life in many different forms. As I am searching for the right words to begin this introduction, I gaze out of the window, where the clouds are passing by quite rapidly today. Being part of the atmospheric boundary layer, the advection of clouds is only one of the numerous examples of turbulent flow. Another one is the cup of coffee standing here in front of me[1]. When adding milk to the coffee, in order to mix the both of them, one usually does not wait until molecular diffusion does its job alone since its time scales are rather large. Inducing turbulence via stirring motion with a spoon, on the other hand, solves the problem. Turbulent transport creates a large interface between the coffee and the milk helping the diffusion process to be completed much faster than in the quiescent case. Besides these everyday-life examples, turbulence is of particular importance to numerous engineering applications, be it in the chemical processing industry, where turbulent flow supports the mixing between different chemicals — as it does for the coffee and the milk —, or in the field of aerodynamics, where turbulent flows around airplanes or cars cause an increase in drag, and thus, fuel consumption. To better understand viscous turbulence in the vicinity of solid walls, many experiments of the three canonical cases of wall turbulence — boundary layer, channel flow, and pipe flow — have been carried out. How essential the pipe flow experiment is in terms of turbulence research was pointed out by Richard Feynman, one of the greatest in physics, as follows:

> *The simplest form of the problem* [of turbulence] *is to take a pipe that is very long and push water through it at high speed. We ask: to push a given amount of water through that pipe, how much pressure is needed?*

[1]The contribution of that substance to the accomplishment of this thesis is highly acknowledged.

> *No one can analyse it from principles and the properties of water. If the water flows very slowly, or if we use a goo thick like honey, then we can do it nicely. You will find that in your textbook. What we really cannot do is deal with actual, wet water running through a pipe. That is the central problem which we ought to solve someday, and we have not.* — Feynman et al. (1963)

Today, we are still unable to solve the problem analytically, but with the aid of the computer resources available now, we can tackle it numerically. In this sense, I hope that the present work will serve as a tiny contribution to a better understanding of fluid turbulence in general. In the following section, the historical background of turbulent flow is further introduced with a special focus on turbulent pipe flow and direct numerical simulation (section 1.1), before the fundamentals of such flow are depicted in section 1.2. Finally, the introduction is closed with the goals and the outline of this thesis (section 1.3).

1.1 Background

The first and probably most famous study of turbulent pipe flow was performed by Reynolds (1883). He injected dye into the centreline of pipe water flow and discovered the onset of turbulence when increasing the flow rate above a certain level. Later, he identified the dependence of the transition to turbulence on a single non-dimensional parameter (Reynolds, 1894), which was then, in his honour, named Reynolds number

$$\mathrm{Re} = \frac{\mathcal{U}\mathcal{L}}{\nu}, \tag{1.1}$$

where $\mathcal{U}$ and $\mathcal{L}$ are the characteristic velocity and the characteristic length scale, respectively, and ν is the kinematic viscosity. The Reynolds number can be interpreted as the ratio between inertial and viscous forces in a fluid flow. With the increase of the Reynolds number, the dye in the pipe flow experiment leaves its shape of a straight line (laminar state) through a transition and becomes completely mixed (turbulent state, $\mathrm{Re} \gtrsim 2000$). The experimental set-up used by Reynolds (1883) as well as his observations of the laminar and turbulent state are depicted in figure 1.1. However, to this day, turbulence has not been clearly defined from a scientific point of view. Frisch (1995), for instance, stresses the ideas of *broken symmetries* and *restored symmetries* when describing the transition to turbulence. A more technical characterisation of turbulence is given by Mathieu and Scott (2000), who describe turbulence through

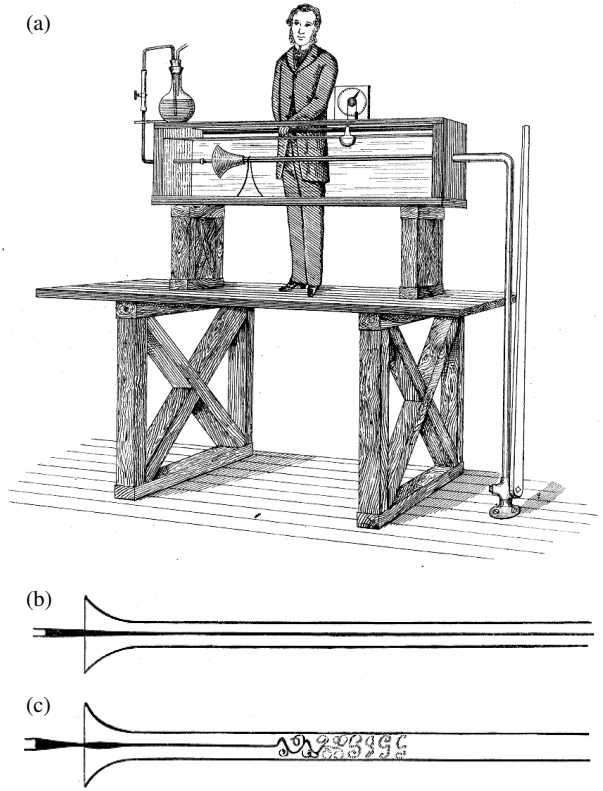

Figure 1.1: Experimental set-up used by Reynolds (1883) (a). Pipe with laminar (b) and turbulent (c) flow state. Figures taken from Reynolds (1883).

its features: *Turbulence is a random process.* Turbulent flows are dependent on space and time involving many degrees of freedom and are therefore unpredictable in detail. Turbulence statistics, however, appear to be reproducible. *Turbulence contains a wide range of scales.* While the largest scales of turbulent motion are determined by the flow geometry, the smallest scales depend on viscosity. As the Reynolds number increases, the range of turbulent scales expands. *Turbulence has small-scale random vorticity.* Space- and time-dependent, intensive, complex vortical motions can be found in turbulent flows with a high Reynolds number. *Turbulence arises at high Reynolds numbers.* The occurrence of turbulence is caused by the instability of a laminar flow. As the Reynolds number rises, the non-linear term of the governing flow equation becomes dominant with respect to the instability-damping viscous term. Hence, the flow tends towards the turbulent state. *Turbulence dissipates energy.* Small-scale turbulent motions cause large local velocity gradients. Consequently, the rate of kinetic energy dissipation into heat, which is proportional to the velocity gradients, is quite high in turbulent flows with respect to laminar flows. In statistically stationary turbulence, energy is continuously supplied to large-scale motions, from which it is transferred towards the smallest scales via the so-called turbulent energy cascade (Richardson, 1922), where it finally dissipates. *Turbulence is a continuum phenomenon.* The smallest scales in the turbulent flows considered in this thesis are some orders of magnitude larger than the molecular mean path. The governing equations describing the motion of fluids are the Navier-Stokes equations, see section 1.2.2. These non-linear equations feature strong sensitivity to small variations in the initial conditions and cannot be solved analytically without drastic simplifications. Due to the increase in the available computational power during the last decades, numerical methods have become important in the field of turbulence research. The most common approaches are referred to as Reynolds-averaged Navier-Stokes (RANS), large-eddy simulation (LES) and direct numerical simulation (DNS). The two first mentioned methods require turbulence modelling, since either only the time-averaged equations are solved, which introduces new unknown correlation terms (RANS), or only the larger turbulent scales are resolved (LES). Only the DNS fully resolves all spatial and temporal turbulent scales and is therefore the most accurate tool to study turbulence on all scales without having to make additional assumptions.

1.1.1 Direct Numerical Simulation

The term DNS was first used by Orszag (1970), who introduced this method to compute the energy spectrum of homogeneous isotropic incompressible turbulence.

DNS is not only the most accurate method of studying turbulence, but also the most expensive computationally, since the computational costs increase as Re^3 (Pope, 2000). Consequently, the first DNSs were restricted to flows with low Reynolds number. In addition to homogeneous turbulent flows with or without imposed mean velocity gradients (Bardina et al., 1985; Lee et al., 1990; Orszag and Patterson, 1972; Rogers and Moin, 1987), inhomogeneous flows such as turbulent boundary layer (TBL) as well as turbulent pipe and plane channel flows have also been subject to DNSs. Here, steep velocity gradients and small-scale motions in the vicinity of the wall require a higher resolution towards the solid boundary. The numerical studies of turbulent plane channel flow performed by Kim et al. (1987), of TBL flow performed by Spalart (1988), and of turbulent pipe flow performed by Eggels et al. (1994) were pioneering DNSs in wall-bounded turbulence and have given us deep insights into the so-called turbulent near-wall cycle (see section 1.2.5). The investigation of the near-wall cycle by means of DNS was later the focus of many studies, i.e. Jeong et al. (1997); Jiménez et al. (2005); Jiménez and Moin (1991); Jiménez and Pinelli (1999).

With the improvement of computational resources, simulations with higher Reynolds numbers became feasible and have been carried out in the last decades. High Reynolds numbers exhibit a broad range of turbulent scales, and it was discovered that not only the small scales related to the near-wall cycle contain energy, but also the large scales located in the logarithmic region. Channel flow DNSs by Abe et al. (2004, 2001); del Álamo and Jiménez (2003); del Álamo et al. (2004); Hoyas and Jiménez (2006); Jiménez et al. (2004) dealt with these large-scale motions and their interaction with the wall — described in more detail in section 1.2.5 — by extending the Reynolds number regime up to $\mathrm{Re}_\tau = 2003$. Please note that this is the friction Reynolds number, which is defined later in equation (1.46). Recently, in order to reach a clear distinction between the small-scale motions (SSMs) near the wall and the large- and very-large-scale motions (LSMs,VLSMs) in the outer layer and to observe a distinguished logarithmic region in plane channel flow, DNSs have been carried out for $\mathrm{Re}_\tau = 5200$ by Lee and Moser (2015) and for $\mathrm{Re}_\tau = 8000$ by Yamamoto and Tsuji (2018). Besides the above-mentioned, the scope of DNSs done on wall-bounded turbulence comprises open channel flows (Handler et al., 1999, 1993; Nagaosa, 1999; Nagaosa and Handler, 2003; Wang and Richter, 2019), open and closed duct flows (Gavrilakis, 1992; Sakai, 2019; Uhlmann et al., 2007), plane Couette flows (Avsarkisov et al., 2014; Lee and Moser, 2018; Pirozzoli et al., 2014), and the turbulent Ekman layer in the planetary atmosphere (Ansorge and Mellado, 2014), amongst other cases. A brief overview of the DNSs of turbulent pipe flow can be found in the next section together with experimental investigations of this flow type.

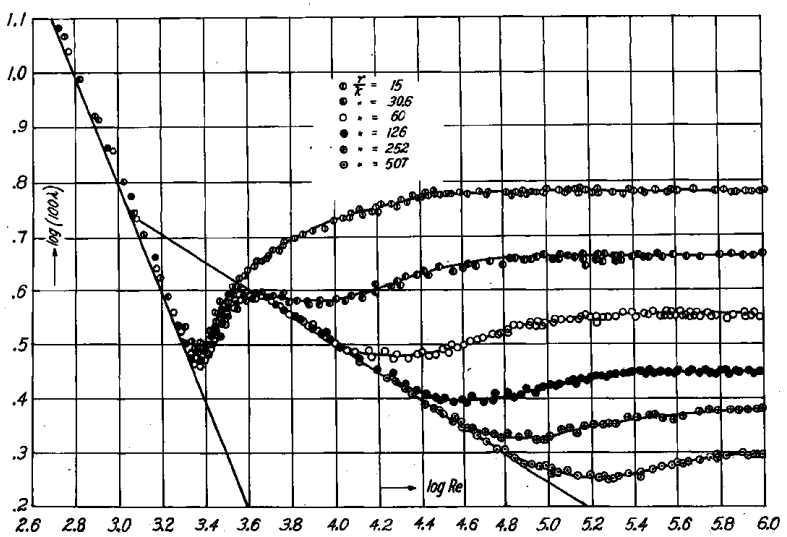

Figure 1.2: Relation between $\log(100\lambda)$ and $\log(\mathrm{Re})$ with λ being the friction factor, k/r the relative roughness and Re the Reynolds number. Figure adapted from NACA technical memorandum 1292, a translation of Nikuradse (1933).

1.1.2 Turbulent Pipe Flow

Pipe flows occur in natural as well as in technical systems. The flow of blood through human vessels is an example of a mostly laminar[2] non-Newtonian pipe flow. Most technical applications, on the other hand, feature turbulent flows of Newtonian fluids. Consequently, the turbulent flow of a Newtonian fluid through a pipe has been the subject of various experimental and numerical studies. After Reynolds (1883), pioneering investigations focussing on friction laws in turbulent pipe flow were carried out by Blasius (1913) and later by Nikuradse (1932, 1933), whose relations between the friction factor, the Reynolds number, and the pipe roughness, as shown in figure 1.2, have become basic knowledge for today's engineering students. Moreover, Nikuradse (1932) was the first to fit the constants of the *logarithmic law of the wall* (or *log law*) by von Kármán (1930) — introduced in section 1.2.5 — into experimental data. While

[2]Indeed, the flow of blood through the vessels of a healthy human being is laminar. Diseases as arteriosclerosis, however, cause a local partial blockage of the vessel, which leads to a turbulent blood flow.

Nikuradse (1933) used an artificial uniform roughness by means of a sand coating in the pipe interior, Colebrook and White (1937) repeated the measurement with non-uniform roughness and derived a friction law for the transition between the smooth and the fully rough regime. Finally, the findings of the studies of Blasius (1913), Nikuradse (1932, 1933), and Colebrook and White (1937) have been visualised in the so-called Rouse diagram (after Rouse (1943)[3]), which also found its way into today's engineering textbooks (see e.g. Schlichting and Gersten (2017)). Henceforth, I only consider the case of a turbulent flow through a smooth pipe, as described in section 1.2.1.

The first detailed measurement of turbulence statistics involving the mean velocity profile, second-, third-, and fourth-order moments of the velocity distribution as well as velocity spectra were performed by Laufer (1954) with the aid of hot-wire anemometry. As the latter study exhibited some inconsistencies regarding the measurement of the dissipation rate, Lawn (1971) later reported a more accurate determination of the dissipation rate in turbulent pipe flow. Patel and Head (1969) measured the log law constants experimentally for both turbulent plane channel and pipe flow. They found the constants to vary between those two types of flow and attributed this to the different geometry. Aiming at the scaling of statistics in turbulent pipe flows, Perry and Abell (1975) carried out detailed measurements over a range of Reynolds numbers ($80000 \leq \mathrm{Re} \leq 260000$) and compared them with previous works. They described an inner and an outer scaling region for turbulence intensities, which is discussed in more detail in section 1.2.5. The scaling of turbulence statistics is closely related to the underlying turbulent coherent structures. Sabot and Comte-Bellot (1976) investigated coherent structures in the core region of turbulent pipe flow by means of a quadrant analysis of the Reynolds shear stress. While the structure of the Reynolds shear stress was found to be similar to the structure in turbulent boundary-layer flow in the vicinity of the wall, this was not the case for the core region. Here, the structures on one side of the pipe axis interacted with the structures from the other side, which produced different results with respect to the turbulent boundary-layer flow. Perry et al. (1986) developed a well-recognised model for wall turbulence including the scaling of turbulence spectra, which they underpinned with pipe flow measurements.

In the 1990s, new measurement techniques, such as laser Doppler anemometry (LDA) and particle image velocimetry (PIV) came into play. Westerweel et al. (1993) and Durst et al. (1995b) worked on highly resolved near-wall measurements of turbulent

[3]The diagram is (in a slightly different form) also referred to as the Moody chart, after Moody (1944). However, although Moodys adaption uses more practicable coordinates (λ and Re instead of $1/\sqrt{\lambda}$ and $\mathrm{Re}\sqrt{\lambda}$), it contains the same information as the original work. Consequently, I prefer to introduce the original Rouse diagram here.

pipe flow with a low Reynolds number by means of PIV and LDA, respectively. These experimental studies were in agreement with plane channel flow DNS (Kim et al., 1987) for statistical moments of the velocity distribution up to fourth order, in general. However, discrepancies were detected for the flatness factor of the radial velocity near the wall, which was not as steep as in the DNS data.

It was not until 1993 that the first DNSs of turbulent pipe flow were performed by Eggels et al. (1993) and Unger (1994). A good comparison between their DNS data of $\mathrm{Re}_\tau = 180$ and both the turbulent pipe flow experiments and the plane channel flow DNS can be found in Eggels et al. (1994). Their work confirmed earlier findings by Patel and Head (1969), who presented different log laws for channel and pipe flow. Most of the turbulence statistics up to fourth order, on the other hand, agreed well between the DNSs of both types of flow. Only the wall-normal skewness factor was found to differ. Eggels et al. (1994) connected this phenomenon to a different "impingement" mechanism close to the curved pipe wall. The high level of wall-normal flatness very close to the wall found in numerical simulations (both channel and pipe) was again absent in the experimental data. Furthermore, the digital PIV study by Westerweel et al. (1996), who experimented on the same Reynolds number case with a new measurement technique, was perfectly in line with earlier experimental studies, and thus, did not recover the high wall-normal flatness level obtained from numerical observations.

One of the biggest controversies in wall-bounded turbulence in the latest history was the question whether the assumptions on which the log law is based are correct, and whether the log law is universal, meaning it stands independent of the Reynolds number. Barenblatt (1993); Barenblatt and Prostokishin (1993) questioned the validity of the log law and proposed a power law of the following form instead

$$u^+ = C \cdot (y^+)^\alpha, \tag{1.2}$$

with the coefficients C and α. To evaluate the different theories of the mean velocity scaling for very high Reynolds numbers, turbulent pipe flow experiments have been carried out in the *superpipe* facility in Princeton, USA, over a wide range of Reynolds numbers. While Barenblatt et al. (1997) argued that the *superpipe* data underpin the theory of a power law, Zagarola et al. (1997) suggested that the data rather support a universal log law for high Reynolds numbers. Figure 1.3 displays the mean velocity profiles measured by Zagarola and Smits (1997) over a range of Reynolds numbers and the log law they fitted. Additionally, Zagarola and Smits (1997) fitted the power law to their data. Both fits led to an accurate representation of the mean velocity

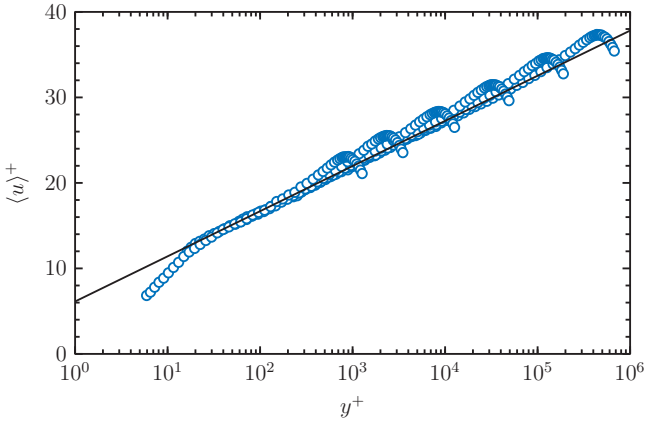

Figure 1.3: Mean velocity profiles of fully-developed turbulent pipe flow. ○, Experimental data of Zagarola and Smits (1997), $\mathrm{Re} \approx 3.2 \times 10^4$, 9.9×10^4, 4.1×10^5, 1.8×10^6, 7.7×10^6, and 2.99×10^7. Solid line, log law $u^+ = 1/\kappa y^+ + B$ with $\kappa = 0.436$ and $B = 6.13$.

profiles. However, while the constant α in the power law depends on the Reynolds number, the constants of the log law are independent of the Reynolds number, which means that the log law is universal. As a consequence, Pope (2000) highlights the practical importance of the log law as compared to the power law. Despite the type of the mean velocity scaling law and its universality, there is an ongoing debate about its range of validity. While the overlap region was initially believed to start around $y^+ \approx 30$, this value has been shifted more and more away from the wall. Accordingly, Zagarola and Smits (1998) suggested that the logarithmic region starts at $y^+ \approx 600$ for high-Reynolds-number pipe flow. Besides, Zagarola and Smits (1998) proposed a power law region located before the log law region in terms of wall distance. Later, McKeon et al. (2004a,b, 2005) repeated the experiment using more accurate measurement techniques and confirmed the findings of Zagarola and Smits (1998) reporting only slightly different log law coefficients. By comparing the superpipe data with data obtained from boundary layer and channel flow experiments, Nagib and Chauhan (2008) discovered the von Kármán coefficient to depend on the flow type, and thus, to be non-universal. Almost a decade later, Luchini (2017) showed that the dependency on the flow type is caused by the effect of the pressure gradient on the mean velocity

profile. Taking this effect into account by means of a higher-order perturbation, he derived a novel universal formulation of the log law.

Another very influential investigation in terms of turbulent pipe flow is the study of Kim and Adrian (1999), who measured long regions of streamwise velocity fluctuations they called VLSMs. These turbulent coherent structures contribute to the turbulent kinetic energy and interact with the small viscous scales in the vicinity of the wall. As a consequence, experimental (Bailey and Smits, 2010; Guala et al., 2006; Hellström et al., 2011; Hellström and Smits, 2014) as well as numerical investigations (Ahn et al., 2013, 2015; Lee et al., 2015; Lee and Sung, 2013; Wu et al., 2012) aimed at a structural characterisation of VLSMs in turbulent pipe flow, which is further described in section 1.2.5. While the first turbulent pipe flow DNSs by Eggels et al. (1993) and Unger (1994) were restricted to Reynolds numbers as low as $\mathrm{Re}_\tau = 180$, the rapid increase of computational resources within the last decades has led to a successive increase in Reynolds numbers in the studies of turbulent pipe flow and turbulent plane channel flow. Wagner et al. (2001) examined the low-Reynolds-number effects in turbulent pipe flow up to $\mathrm{Re}_\tau = 320$, before Wu and Moin (2008) carried out pipe flow DNS up to $\mathrm{Re}_\tau = 1142$. Whereas the latter studies involved second-order schemes for the spatial and temporal discretisation, Boersma (2011, 2013) computed velocity statistics up to $\mathrm{Re}_\tau = 1842$ in fully-developed turbulent pipe flow using a pseudo-spectral method, and El Khoury et al. (2013) used a spectral-element method for pipe flow DNS up to $\mathrm{Re}_\tau = 1000$. Recently, Ahn et al. (2017, 2013, 2015), Lee and Sung (2013), and Lee et al. (2015) have carried out turbulent pipe flow DNSs using a second-order, finite-difference scheme and have extended the regime of Reynolds numbers accessible by DNSs up to $\mathrm{Re}_\tau = 3008$.

The debate whether the mean velocity profile follows a log law or a power law, as well as the investigation of the interaction of VLSMs with the near-wall turbulence, calls for highly-resolved, high-Reynolds-number experiments. Since the above-described experiments were performed in the Princeton superpipe facility, several additional facilities for turbulent pipe flow experiments have been set up — such as the Cottbus large pipe test facility in Germany (CoLaPipe, König et al., 2014; Öngüner, 2018), the high-Reynolds-number flow facility in Japan (Hi-Reff, Furuichi et al., 2015), and the centre for international cooperation in long pipe experiments in Italy (CICLoPE, Fiorini, 2017; Talamelli et al., 2009). Thanks to its large diameter ($D = 0.9\,m$), the CICLoPE facility is capable of measuring the smallest turbulent scales even for high-Reynolds-number flows, see figure 1.4. Recently, researches have been conducted in this facility studies regarding the scaling of turbulent fluctuations (Örlü et al., 2017; Willert et al.,